

P8.27 SURFACE OBSERVATIONS OF THE REAR-FLANK DOWNDRAFT EVOLUTION ASSOCIATED WITH THE AURORA, NE TORNADO OF 17 JUNE 2009

Bruce D. Lee¹, Catherine A. Finley¹, Christopher D. Karstens², and Timothy M. Samaras³

¹ WindLogics, Inc., Grand Rapids, MN

² Iowa State University, Ames, IA.

³ National Technical Systems, Littleton, CO.

1. Introduction

During the 2009 field season of the Tactical Weather-Instrumented Sampling in/near Tornadoes Experiment (TWISTEX), a mobile mesonet (Straka et al. 1996) collected evolutionary near-surface observations across the hook echo region of a cyclic tornadic supercell that occurred near Grand Island and Aurora, NE on 17 June 2009. Of particular interest, the mesonet collected data across the hook echo region over nearly the full lifecycle of the Aurora tornado that lasted 23 min. The observations included sampling in the rear-flank downdraft (RFD) outflow both west and east of the tornado, including extended observations by part of the mesonet in close proximity to the tornadogenesis and tornado regions. This dataset has provided the opportunity to examine the evolution of portions of RFD outflow, including the near-tornado environment, over most of the lifecycle of a significant tornado.

For perspective, although a substantial number of mobile mesonet RFD outflow datasets have been collected and analyzed over the past approximately 17 years to determine the association between RFD outflow thermodynamic and kinematic character and the tornadic nature of a supercell (e.g., Markowski et al. 2002, hereafter MSR2002; Grzych et al. 2007, hereafter GLF2007; Hirth et al. 2008; Lee et al. 2010), there exist comparatively few RFD outflow mesonet datasets with sampling within very close range of a tornado (e.g., Finley and Lee 2004, 2008; Lee et al. 2010). Rarer still are mesonet evolutionary datasets within the RFD of tornadic supercells as in Lee et al. (2004) and Hirth et al. (2008). The reason for the rarity of these types of datasets

involves the difficulty of getting a tornadic supercell with modest storm motion into a good road network while strategically positioning a mobile mesonet or set of StickNet arrays (Weiss and Schroeder 2008). In addition to emphasizing field agility in the project makeup, a major motivation for conducting ongoing TWISTEX spring field operations is to increase the number of opportunities for obtaining these rare datasets.

TWISTEX 2009 was conducted during May and June with a domain that included regions from the Upper Midwest through the southern Great Plains. The project had a typical complement of four mobile mesonet vehicles with one of the teams transporting an array of in situ probes (see Karstens et al. 2010, their Fig. 3). The primary objective of the field portion of TWISTEX was to gather thermodynamic and kinematic data with a mobile mesonet in the RFD outflow region near tornadoes and the adjacent RFD gust front (RFDGF) region, while concurrently gathering thermodynamic data with in situ probes in or very near tornadoes. The sampling goal was designed such that a combined thermodynamic and kinematic characterization and mapping could be done in the tornadogenesis and tornado maintenance regions while also addressing project objectives involving near-surface tornadic flow field analysis with the aid of the video probes.

2. Event Overview and Storm Environment

The targeted supercell, hereafter referred to as the Aurora storm, developed near the intersection of a west-east oriented stationary front and northwest-southeast positioned outflow boundary. Convective initiation was near 2218 UTC northwest of Kearney, NE with the cell exhibiting persistent supercell characteristics by approximately 2347 UTC based on National Weather Service WSR-88D radar at Hastings, NE (UEX). Although the Aurora storm produced at least two short-lived tornadoes over the next half

Corresponding author address: Dr. Bruce D. Lee
WindLogics, Inc. – Itasca Technology Center
Grand Rapids, MN 55744
email: blee@windlogics.com

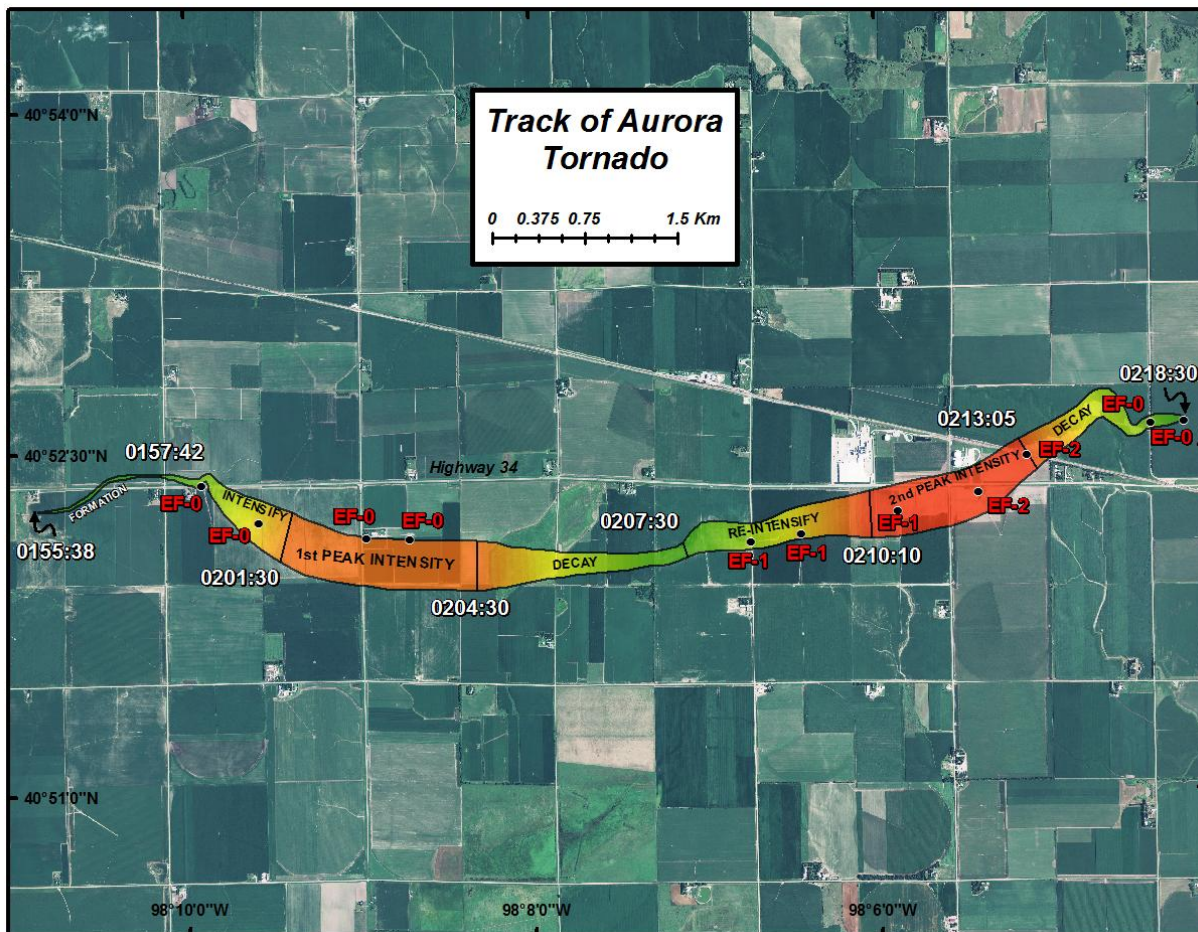


Fig. 1. Track of the Aurora tornado. Shaded areas indicate transitions in tornado intensity. Times corresponding to changes in tornado intensity shown in white. NWS damage indicators marked with black dots.

hour, the storm did not produce a tornado of substantial strength and duration until 0155:40 UTC 15 km west of Aurora. The Aurora tornado produced EF-2 damage (NCDC 2009); however, its path largely remained over agricultural land with only a few structures impacted as shown in the reconstructed tornado path of Fig. 1. Using numerous sources which included the Hastings National Weather Service damage survey, National Climatic Data Center records, extensive videography, and aerial orthophotos fortuitously taken after this event, the path dimensions were reconstructed as well as lifecycle stages inferred (see Karstens et al. 2010 for details regarding this reconstruction). The tornado had a peak width of 430 m with a path length of 10.1 km.

To assess the convective environment the Aurora storm was moving into, the sounding

shown in Fig. 2 was created using Rapid Update Cycle (RUC) model (Benjamin et al. 2004) analysis data at 0100 UTC on June 18. Using mobile mesonet inflow data for the sounding surface conditions, the 50 mb mixed layer CAPE and CIN are 3632 J kg^{-1} and -44 J kg^{-1} , respectively. Storm-relative helicity through the 0-3 km layer is $367 \text{ m}^2 \text{ s}^{-2}$, with nearly half of this value, $166 \text{ m}^2 \text{ s}^{-2}$, residing in the 0-1 km layer. The Energy Helicity Index combined thermodynamic-shear parameter was 3.9 in the 0-1 km layer. These indices along with a low lifted condensation level of 658 m reflect a convective environment favorable for tornadic supercells (Rasmussen and Blanchard 1998; Rasmussen 2003; Thompson et al. 2003).

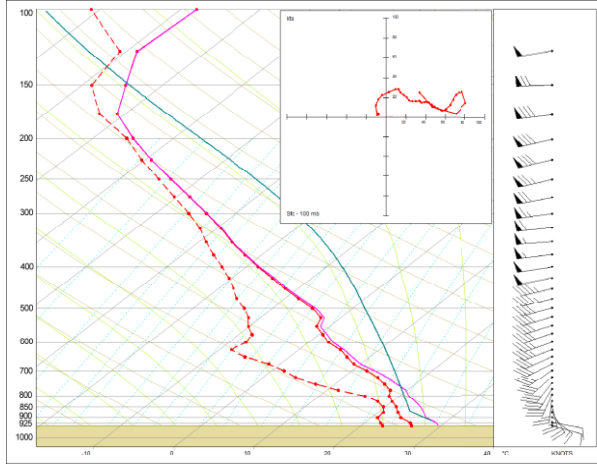


Fig. 2. 0100 UTC storm inflow sounding with hodograph inset. 50 mb mixed layer parcel ascent path (green) with virtual temperature correction shown.

3. Data Collection and Methodology

The modest easterly storm motion ($\sim 9 \text{ m s}^{-1}$) down U.S. Highway 34 between Grand Island and Aurora afforded the project the option of mesonet sampling in roughly consistent storm-relative locations over most of the tornado life. This strategy trades the opportunity for broader area mesonet coverage within the RFD/hook region of the supercell for tighter storm-relative positioning more conducive for evolutionary analysis. For the analysis presented here, the data collected during the period from 0150:00 - 0218:30 will be used. Note that the tornado was in progress between 0155:40 and 0218:30 UTC. As will be apparent in the spatial analysis plots to follow, most of the sampling took place along HW 34 that bisected the low-level mesocyclone and hook regions of the storm. Optimal sampling for this operation called for a team west of the tornado in the 2-4 km range, a team east of the tornado doing transects through the RFD gust front (RFDGF) and internal boundaries, one team south of the tornado and one team (the in situ probe deployment team) sampling the region in very close proximity to the tornado. Most of these sampling goals were met with the exception of the team designated south of the tornado. The vast influx of storm observers into the area compromised project real-time cellular data vehicle/radar tracking communications, and at times, hampered team movement. These in-field challenges resulted in only late coverage south of the tornado path; however, sampling along the west-east cross-section was enhanced with the "southern team"

taking data in the 1-3 km region just east of the tornado.

Mesonet data went through quality control and bias correction procedures similar to that outlined in MSR2002 and GLF2007. Given the mesoscale nature of the storm environment, the mobile mesonet was utilized to determine the base state used to assess perturbation quantities of thermodynamic variables. Periods were selected when one of the mesonet teams was sampling air with a thermodynamic character deemed to be representative of the pre-storm environment.

Data points were plotted relative to the UEX WSR-88D radar base reflectivity data using time-to-space conversion as described by MSR2002. This process put the mesonet data into the storm's positional frame of reference. Given the short time period over which substantial changes in the thermodynamic and kinematic fields can occur in any storm-relative location, we utilized 3 min data samples (1.5 min either side of a reference time). The analysis times are time-space referenced to the nearest radar time. Five second averages are used for all analysis.

4. Observations and Analysis

The Aurora supercell presented classic structure both in the field and on radar. Figure 3 presents the radar evolution over the primary analysis period and provides perspective for the close-up hook echo regions used in the spatial analysis plots. Given the classic supercell structure and fortunate team deployment locations, only very late in the deployment did any team experience rainfall at a rate higher than moderate intensity (and that was for only approximately 1 min). As shown in Fig. 4 for a three minute analysis time centered on 0154:30 UTC, teams are arrayed out across the hook region and collectively resolve a large buoyancy gradient across the hook as manifest in a 4-5 K spatial difference in θ_v deficits. Only modest negative buoyancy exists in the tornadogenesis and near-tornado region, with θ_v deficits of 0 - 2 K, typical of those seen in "warm" RFD outflows of tornadic supercells (MSR2002; GLF2007).

A noteworthy aspect of this first analysis period is the internal RFD surge encountered by part of the mesonet east of the eventual tornadogenesis location. The RFD outflow surge (RFDOS), internal to the RFDGF as shown in Fig. 4, reaches the teams within 3 min of tornadogenesis time at 0155:38 UTC (reference location in Fig. 1 and image in Fig. 5). This RFDOS was accompanied by only weak negative buoyancy as noted above. The association

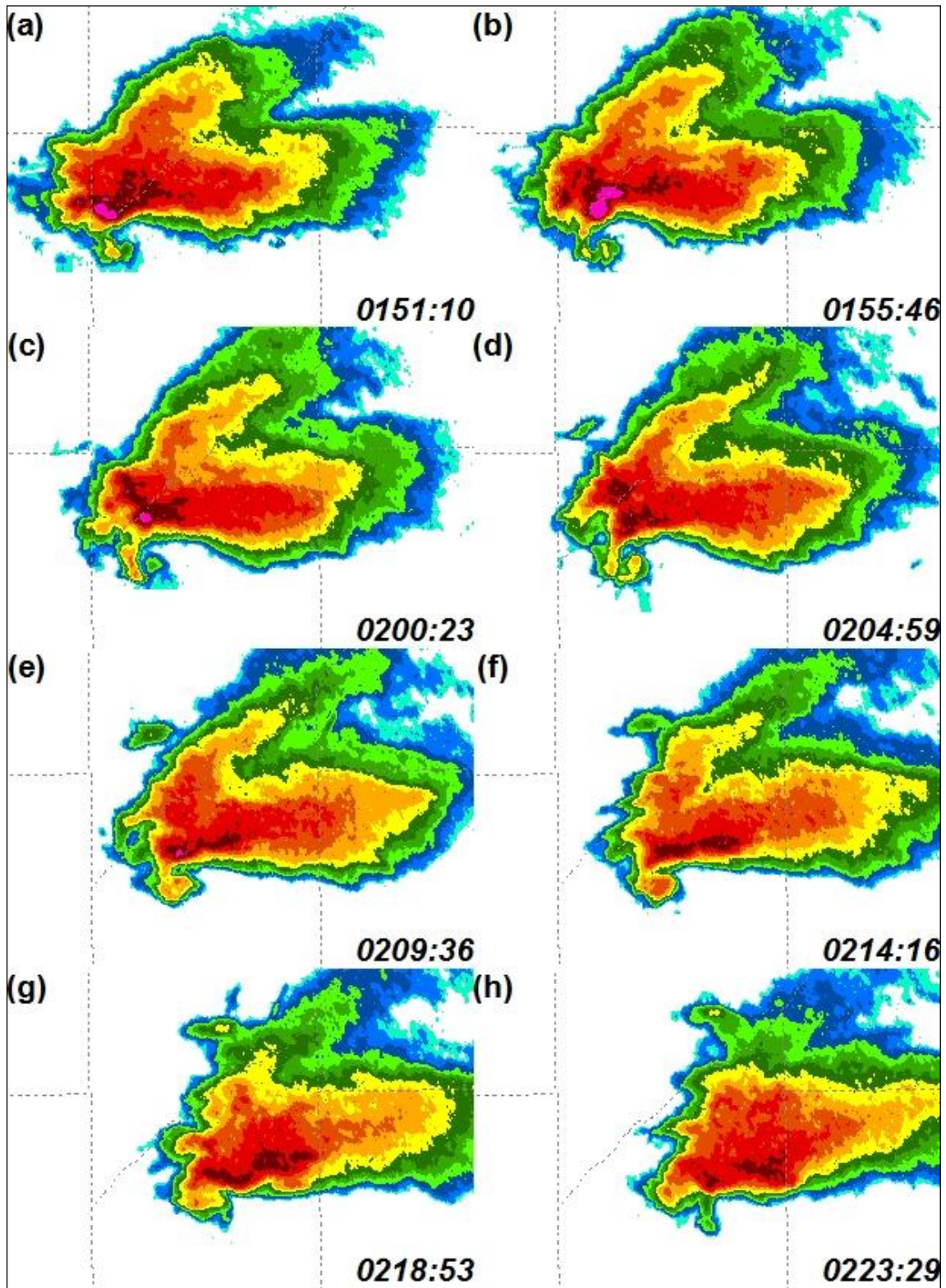


Fig. 3. UEX WSR-88D base reflectivity at 0.5° tilt of the Aurora supercell.

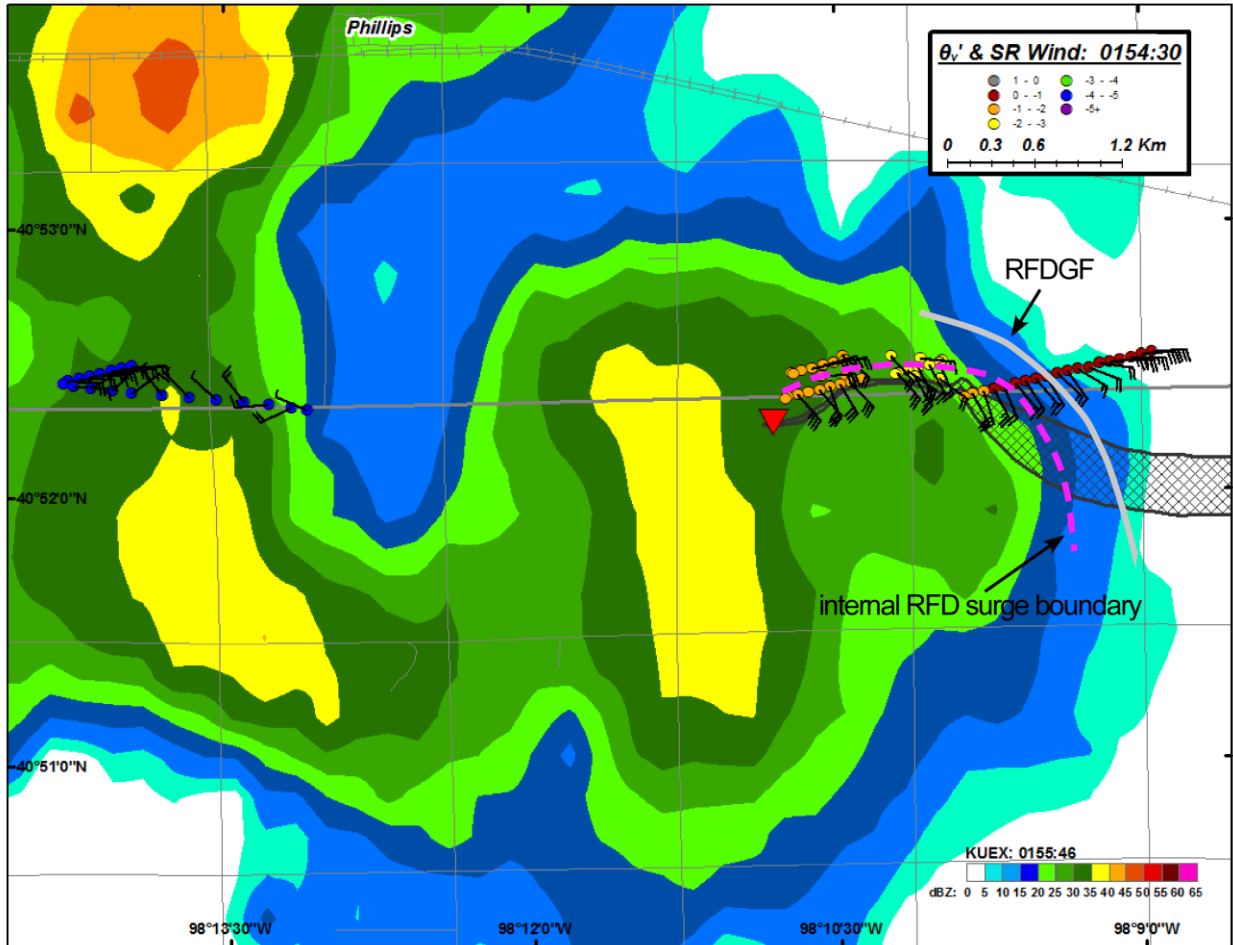


Fig. 4. Mesonet data overlaid on UEX radar reflectivity imagery with time-space conversion applied. Data spans a 3 min period centered on 0154:30 UTC. Observations of θ_v' (K) and storm-relative winds are shown. Half barb, full barb and flag on wind staff are 2.5 m s^{-1} , 5 m s^{-1} and 25 m s^{-1} , respectively. Data are separated by 10 s. Stations with no staff had wind data removed in quality control. Some overlapping station data (early) removed for clarity. See color coding in the legend for θ_v' .

between the RFDOS and tornadogenesis may be similar to that documented for the Bassett, NE tornadic supercell (Finley and Lee 2004) and the Quinter, KS tornadic supercell (Finley and Lee 2008), the latter of which was accompanied by a particularly intense RFDOS that was associated with the formation of a very large tornado. Additional evidence in both mesonet and radar data is mounting regarding the occurrence of the RFDOS and/or its leading edge boundary near tornadoes (e.g., Marquis et al. 2008a, b; Lee et al. 2010).

Consistent but more pronounced than in θ_v' , the west-east gradient in θ_e' across the hook is very large ($\sim 20 \text{ K}$) as shown in Fig. 6. In contrast to the relatively modest θ_v' deficits near the



Fig. 5. Initial tornado formation at 0155:38 UTC as viewed from the east by M3.

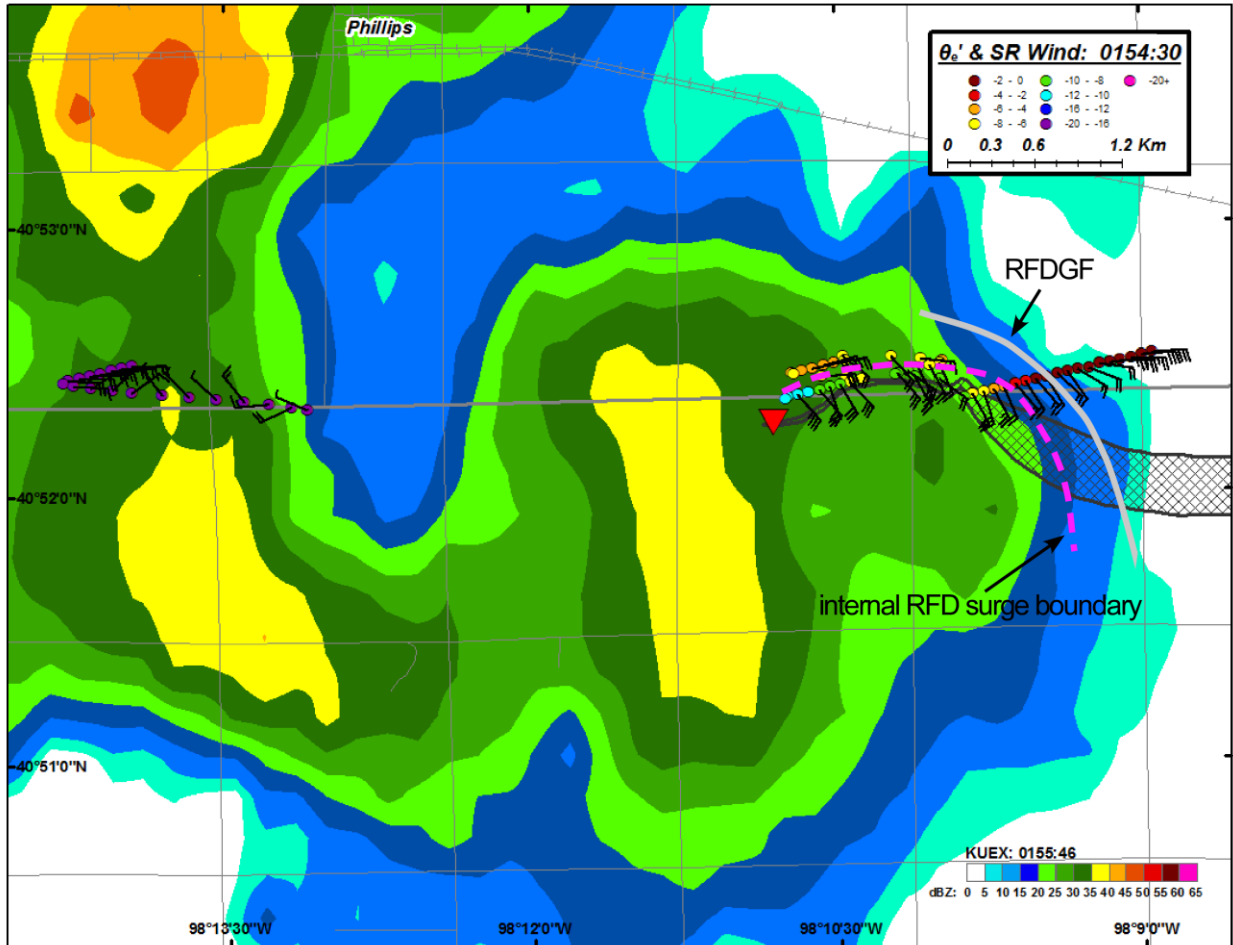


Fig. 6. As in Fig. 4 except for θ_e '.

tornado, the θ_e deficits range from moderate just north of the tornado/tornadogenesis area to quite large (> 10 K) behind the RFDOS boundary. These large θ_e deficits run counter to typical values found in tornadic supercell RFD outflows that were usually < 4 K (MSR2002, GLF2007).

The tornado remained visually weak up to around 0157:42 UTC (see Fig. 1) after which, ground rotation intensity began increasing. Tornado intensification was marked starting at about 0159:00 UTC. Of interest was the RFDOS developing to the southwest and south of the tornado that was concurrent with this distinct intensification stage. As shown in Fig. 7, an RFDOS was moving through mesonet team MT at 0158:10 UTC. Westerly storm-relative winds exceeded 19 m s^{-1} within the next approximate half minute (peak unaveraged ground-relative wind speed reached 30 m s^{-1}). Around 0159:50 UTC, strong outflow from this surge began lofting large quantities of soil from the agricultural fields just south of the tornado as documented in Fig. 8. A much larger tornado was apparent after this

intensification stage (Fig. 9).

Slightly less buoyant air is present within the near-tornado region as shown in Fig. 7, although the θ_v deficits are still only modest (2 - 3 K range). Deficits in θ_e near the tornado region (not shown) remain large with values commonly greater than 8 K. The contrasting signals between θ_v and θ_e deficits is a striking characteristic of this dataset throughout the sampling period, along with the very large west-east gradient in both θ_v and θ_e across the hook. The RFDOS possessed air with similar buoyancy to the air that preceded it, but markedly cooler θ_e values.

During most of the tornado life, substantial potential buoyancy existed near the tornado, even with large θ_e deficits. Mesonet observations were inserted into the inflow sounding to calculate surface-based CAPE (and CIN). As shown in Fig. 10 for the 0201:56 UTC analysis time, CAPE values in the tornado proximate area are considerable with CAPE in the $1500 - 2500 \text{ J kg}^{-1}$ range. CIN ranged from $130 - 240 \text{ J kg}^{-1}$.

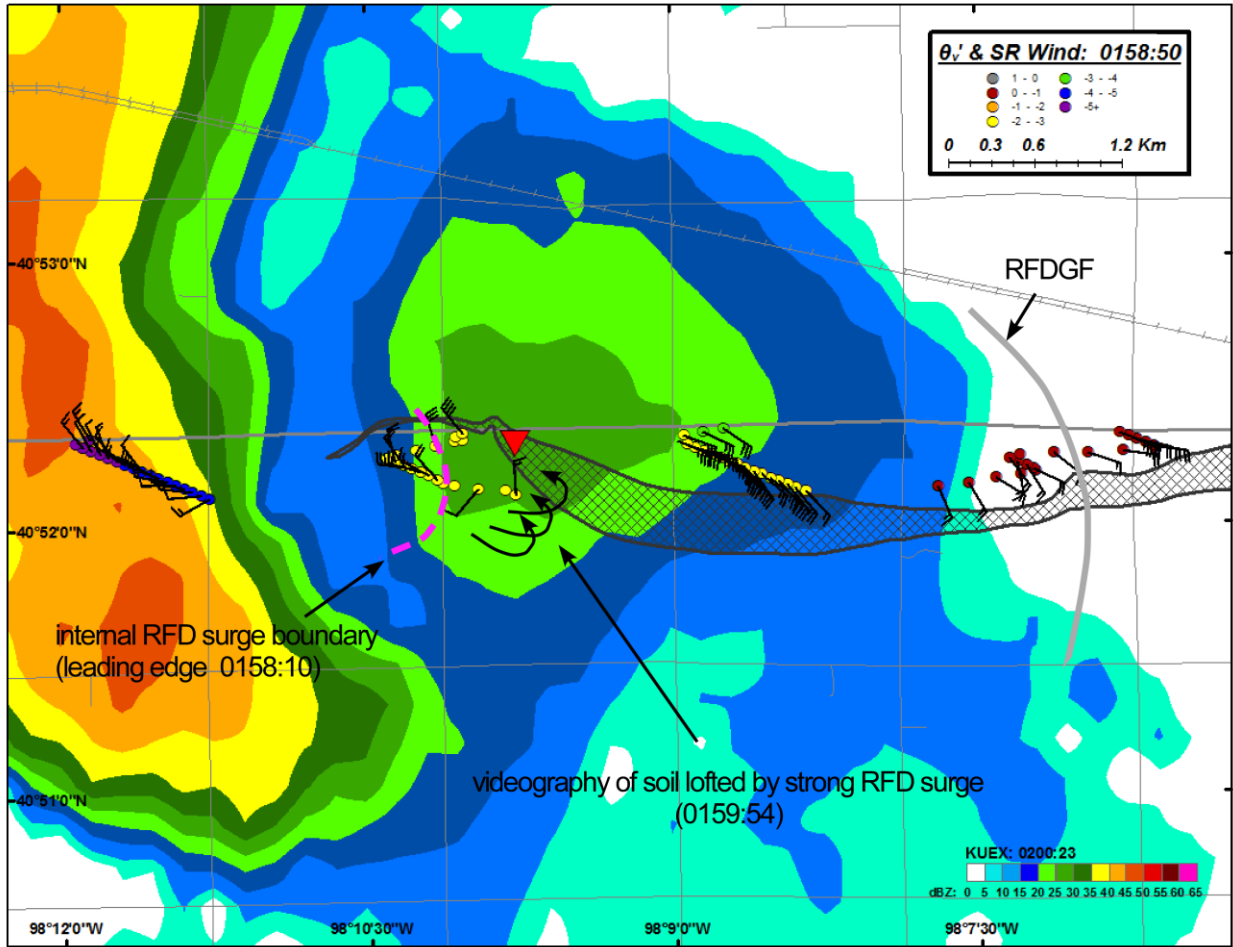


Fig. 7. As in Fig. 4 except for analysis center time of 0158:50 UTC.



Fig. 8. Lofted soil by strong RFDOS at 0159:54 UTC as viewed from the east by M2.



Fig. 9. Aurora tornado as viewed from the west by M1 at 0202:55 UTC.

During much of this analysis time an arc of downdraft was observed bounding the southern flank of the tornado (quite apparent in time-lapsed videography). Additionally, a persistent near-surface inflow jet was observed south of the tornado that clearly delineated parcel paths directed into the tornado over a depth of a few 10s of meters from the RFD outflow region.

In addition to further spatial analysis, complementary time-series analysis has been completed to identify the temporal-spatial signals characterizing the RFD and tornado proximate environment associated with Aurora tornado. This analysis will be presented at the conference.

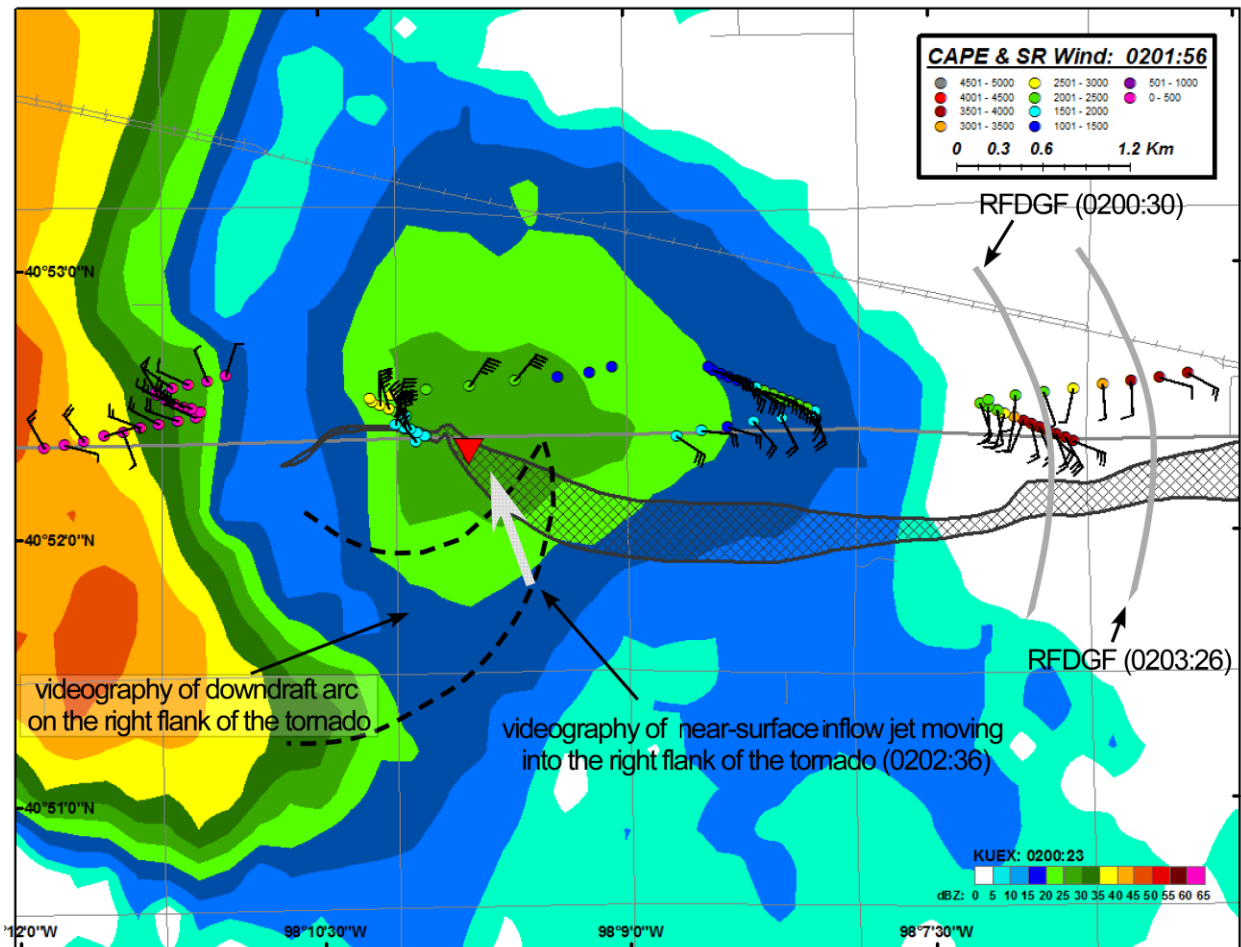


Fig. 10. As in Fig. 4 except for CAPE ($J kg^{-1}$) at analysis center time of 0201:56 UTC.

5. DISCUSSION

The dataset TWISTEX gathered on 17 June 2009 near Aurora, NE represents a rare opportunity to assess the evolution of the surface thermodynamic and kinematic characteristics of air parcels within the RFD outflow and in the immediate vicinity (much of which also technically was in RFD outflow) of a relatively long-lived tornado. Easterly storm motion at moderate speeds with the mesocyclone moving down U.S. HW 34 allowed the mesonet to maintain a sampling cross-section through the Aurora storm hook echo from before tornadogenesis through the late-mature stage of the tornado. On three occasions, a RFDOS accompanied either tornadogenesis or episodes of marked tornado intensification. In addition to the mesonet sampling, extensive videography was very useful for developing a chronology of the mesocyclone and sub-mesocyclone scale morphology.

Over the course of this tornado event, the mesonet cross-section revealed striking contrasts in RFD outflow internal variability. To the west of the tornado, generally in the 2-5 km range, RFD outflow remains quite negatively buoyant with large θ_v deficits (> 4 K). Very large θ_e deficits (often > 16 -20 K) also exist in this region. The evolutionary stability of this thermodynamic partitioning is striking, as up to the late mature tornado stage, there is no evidence that parcels in this region just a few kilometers west of the tornado are moving into the tornado proximate area. In the region within 1-2 km from the tornado, air parcels possess only modest negative buoyancy with θ_v deficits generally less than 2.5 K (most often < 2 K) up to the late mature tornado stage. In this same region, a large inconsistency exists between parameter-relative deficits in θ_v and θ_e . Although the θ_v deficits in this region were generally consistent with typical values found in MSR2002 and GLF2007 for RFD outflows associated with tornadoes, θ_e deficits are not, as they generally remain larger than 8K through the evolutionary sampling.

A major signal from the heterogeneous character of θ_e throughout the hook region infers substantial differences in the altitude from which parcels descended within the RFD. The next part of this study will examine the respective levels on the inflow sounding that have similar θ_e as in various RFD outflow regions. Related to this topic, the video evidence is compelling regarding the source of parcels entering the tornado from

the RFD outflow on the right (southern) flank of the tornado. Analysis of this case is continuing with far more details to be presented in a formal publication in the near future.

6. ACKNOWLEDGEMENTS

Partial support for author Karstens was provided by NOAA grants NA06OAR4600230, NA08OAR4600887, and NA09OAR4600222. The authors thank all TWISTEX 2009 participants for their contributions. Matt Grzych is recognized for his large field systems technical contribution. Tony Laubach is acknowledged for his efforts in compiling and organizing the substantial media archive for TWISTEX. We thank Patrick Skinner for his helpful consultation on data quality control and instrumentation. WindLogics Inc. provided publications support for this work.

7. References

- Benjamin, S. G., D. Dévényi, S. S. Weygandt, K. J. Brundage, J. M. Brown, G. A. Grell, D. Kim, B. E. Schwartz, T. G. Smirnova, T. L. Smith and G. S. Manikin. 2004: An hourly assimilation-forecast cycle: The RUC. *Mon. Wea. Rev.*, **132**, 495–518.
- Finley, C. A., and B. D. Lee, 2004: High resolution mobile mesonet observations of RFD surges in the June 9 Basset, Nebraska supercell during project answers 2003. Preprints, *22nd Conf. on Severe Local Storms*, Hyannis, MA, Amer. Meteor. Soc., Conference CD-ROM,. P11.3.
- Finley, C. A., and B. D. Lee, 2008: Mobile mesonet observations of an Intense RFD and multiple gust fronts in the May 23 Quinter, Kansas tornadic supercell during TWISTEX 2008. Electronic proceedings, *24th Conf. on Severe Local Storms*, Savannah, GA Amer. Meteor. Soc., P3.18.
- Grzych, M. L., B. D. Lee, and C. A. Finley, 2007: Thermodynamic analysis of supercell rear-flank downdrafts from Project ANSWERS. *Mon. Wea. Rev.*, **135**, 240-246.
- Hirth, B. D., J. L. Schroeder, and C. C. Weiss, 2008: Surface analysis of the rear-flank downdraft outflow in two tornadic supercells. *Mon. Wea. Rev.*, **136**, 2344-2363.

- Karstens, C. D., T. M. Samaras, B. D. Lee, W. A. Gallus, and C. A. Finley, 2010: Near-ground pressure and wind measurements in tornadoes. *Mon. Wea. Rev.*, **138**, 2570-2588.
- Karstens, C. D., T. M. Samaras, W. A. Gallus, C. A. Finley, and B. D. Lee, 2010: Analysis of near-surface wind flow in close proximity to tornadoes. Preprints, *25th Conf. on Severe Local Storms*, Denver, CO, Amer. Meteor. Soc., P10.12.
- Lee, B. D., C. A. Finley, and T. M. Samaras, 2010: Surface analysis near and within the Tipton, Kansas Tornado of 29 May 2008. *Mon. Wea. Rev.*, (available at <http://journals.ametsoc.org/doi/pdf/10.1175/2010MWR3454.1>)
- Lee, B. D., C. A. Finley, and P. Skinner, 2004: Thermodynamic and kinematic analysis of multiple RFD surges for the 24 June 2003 Manchester, South Dakota cyclic tornadic supercell during Project ANSWERS 2003. Preprints, *22nd Conf. on Severe Local Storms*, Hyannis, MA, Amer. Meteor. Soc., CD-ROM, 11.2.
- Markowski, P. M., J. M. Straka, and E. N. Rasmussen, 2002: Direct surface thermodynamic observations within the rear-flank downdrafts of nontornadic and tornadic supercells. *Mon. Wea. Rev.*, **130**, 1692-1721.
- Marquis, J. M., Y. Richardson, J. Wurman, and P. Markowski, 2008a: Single- and dual-Doppler analysis of a tornadic vortex and surrounding storm-scale flow in the Crowell, TX, supercell of 30 April 2000. *Mon. Wea. Rev.*, **136**, 5017-5043.
- Marquis, J. M., Y. Richardson, J. Wurman, P. Markowski, and D. Dowell, 2008b: Mobile radar observations of tornadic supercells with multiple rear-flank gust fronts. Preprints, *24th Conf. on Severe Local Storms*, Savannah, GA Amer. Meteor. Soc., paper 19.3.
- NCDC, 2009: *Storm Data*. Vol. 51, No. 6, 982 pp. [Available from National Climatic Data Center, 151 Patton Ave., Asheville, NC 28801.]
- Rasmussen, E. N., 2003: Refined supercell and tornado forecast parameters. *Wea. Forecasting*, **18**, 530-535.
- Rasmussen, E. N., and D. O. Blanchard, 1998: A baseline climatology of sounding-derived supercell and tornado forecast parameters. *Wea. Forecasting*, **13**, 1148-1164.
- Straka, J. M., E. N. Rasmussen, and S. E. Fredrickson, 1996: A mobile mesonet for fine-scale meteorological observations. *J. Atmos. Oceanic Technol.*, **13**, 921-936.
- Thompson, R. L., R. Edwards, J. A. Hart, K. L. Elmore, P. Markowski, 2003: Close proximity soundings within supercell environments obtained from the Rapid Update Cycle. *Wea. Forecasting*, **18**, 1243-1261.
- Weiss, C. C., and J. L. Schroeder, 2008: The 2007 and 2008 MOBILE Experiment: Developing and testing of the TTU StickNet platforms. Preprints, *24th Conf. on Severe Local Storms*, Savannah, GA Amer. Meteor. Soc., paper 5.1.